Optical Interference in Magneto-optic Kerr-effect Measurements of Magnetic Multilayers

G. Mankey – University of Alabama

et al.

Citation of published version:

Maat, S., et al. (1999): Optical Interference in Magneto-optic Kerr-effect Measurements of Magnetic Multilayers. *Journal of Applied Physics*, 85(3).
DOI: https://doi.org/10.1063/1.369301

Optical interference in magneto-optic Kerr-effect measurements of magnetic multilayers

Cite as: Journal of Applied Physics **85**, 1658 (1999); https://doi.org/10.1063/1.369301
Submitted: 23 July 1998 . Accepted: 26 October 1998 . Published Online: 15 January 1999

S. Maat, L. Shen, C. Hou, H. Fujiwara, and G. J. Mankey

Optical interference in magneto-optic Kerr-effect measurements of magnetic multilayers

S. Maat, L. Shen, C. Hou, H. Fujiwara, and G. J. Mankey[a)]
Department of Physics and Astronomy and Center for Materials for Information Technology, The University of Alabama, Tuscaloosa, Alabama 35487

(Received 23 July 1998; accepted for publication 26 October 1998)

Hysteresis loops of exchange-biased permalloy/$Fe_{50}Mn_{50}$/permalloy trilayers on glass were measured as a function of $Fe_{50}Mn_{50}$ and permalloy thicknesses with the longitudinal Kerr effect employing a coherent light source. Kerr signals originate from both permalloy layers and give a superposition of hysteresis loops. In vibrating sample magnetometer or looptracer measurements the contribution of a particular layer to a major hysteresis loop cannot be identified. With the Kerr setup presented it is possible to identify the contribution of each layer individually, since the finite optical path through the trilayer gives rise to optical attenuation and interference. For an increasing total thickness of the trilayer, the signal of the buried permalloy layer will become weaker due to attenuation. Kerr measurements of trilayers up to 40 nm show a superposition of two equally oriented loops. Major loops for trilayers of thickness greater than 40 nm show a superposition of two oppositely oriented hysteresis loops. The transition is dependent only on the total thickness of the trilayer, rather than the thickness of each individual layer. This unusual effect can be explained by the phase difference of the two Kerr signals. Additional measurements performed from the glass side of the samples and measurements of a $Fe_{50}Mn_{50}$/permalloy bilayer confirm that the sense of a hysteresis loop can change for a buried layer due to optical effects. © *1999 American Institute of Physics.* [S0021-8979(99)06903-0]

I. INTRODUCTION

In a spin valve structure, a pinned ferromagnetic (F) layer is exchange coupled to an antiferromagnetic (AF) layer such as γ-FeMn.[1] Fundamental properties such as anisotropy of each layer and exchange coupling determine the performance of these devices. These properties are known to depend on the thickness of both F and AF layers as well as the order in which F and AF layers are deposited,[2] so that measured quantities like coercivity and pinning field will vary. The study of the magnetic switching behavior of trilayers of an AF sandwiched between F layers should provide insight into how the magnetic structure of the AF layer is affected by the F layers. The magneto-optic Kerr effect (MOKE) can be used to study the magnetic hysteresis behavior of these trilayers.

One way to measure the switching of individual F layers is to tune the wavelength of the incident radiation to a value where the Kerr rotation or ellipticity of one of the multilayer components is zero and to analyze the signal of the remaining layers.[3,4] Alternatively, a coherent light source can be employed and optical attenuation and interference are helpful to identify the switching of the individual F layers. In this experiment, the switching of the individual layers is extracted from the magnitude and sign of the MOKE signal.

In the thin film limit, $(2\pi/\lambda)d \ll 1$, where d is the total film thickness and λ is the wavelength of the light, the Kerr signal may be regarded as the sum of the magneto-optical responses from each magnetic layer. For thicker multilayer structures, it is necessary to consider the finite optical path length in the material since the light is strongly attenuated and a phase difference of signals from each layer is accumulated. A calculation of the total Kerr signal from multilayer structures can be performed using Jones matrix formalism.

II. EXPERIMENT

MOKE was used to study the magnetization behavior of trilayers of permalloy ($Ni_{80}Fe_{20}$)/$Fe_{50}Mn_{50}$/permalloy. The trilayer samples were prepared by magnetron sputter deposition on glass substrates with a magnetic field of 40 G applied during deposition to impose a pinning direction for the ferromagnetic permalloy layers. First, a seed layer of 4 nm of Ta was deposited to give the bottom permalloy layer a $\langle 111 \rangle$ texture.[5,6] $Fe_{50}Mn_{50}$ layers were deposited on the bottom permalloy layer. $Fe_{50}Mn_{50}$ grows pseudomorphic on permalloy in the antiferromagnetic γ-fcc phase in the thickness range of our experiments.[7] The Néel temperature of such a layer is around 500 K so no cooling was necessary to impose an exchange bias field.[8] A second permalloy layer was then grown on top of the $Fe_{50}Mn_{50}$ and all samples were capped with 4 nm of Ta to prevent oxidation.

Since the films magnetize in-plane, the longitudinal Kerr effect setup is utilized with the field applied in the plane of incidence. The coils of the used electromagnet restrict the angle of incidence from $\alpha = 0°$ to 50°. Since the amplitude of the longitudinal Kerr effect is roughly proportional to $\sin 2\alpha$, the angle of incidence was chosen to be 45°. The magnetic field was applied in the optic plane. A modulation technique proposed by Nederpel and Martens was used.[9] *p*-polarized

a)Electronic mail: gmankey@mint.ua.edu

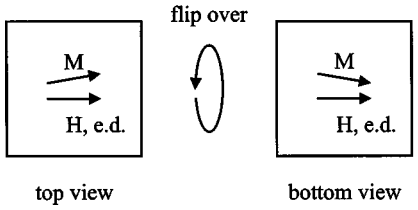

FIG. 1. When the sample is flipped over the easy unidirectional axis (labeled e.d. and the external applied field H do not change orientation. Since only the component of the magnetization of M along H is measured in a hysteresis loop, both measurements can be compared directly.

light from an 8 mW laser diode at 635 nm is used as the light source. The incident light is modulated at a frequency of $f=50.1\,\mathrm{kHz}$ with a photoelastic modulator (PEM). The axis of the PEM is set at 45° with respect to the *p*-polarization axis, so that both the *p* and *s* components of the incident light are modulated. The *p*-polarized component of the reflected light at the fundamental frequency of the modulation is measured with a photodiode and a lock-in amplifier.

The samples were mounted on a rotary table, enabling hysteresis loops to be acquired for angles between the applied field and the pinning direction. With this arrangement, the pinning direction of the F layers can be determined accurately. The magnetic field was swept at 0.1 cycles/s and each hysteresis loop was averaged over 10 field cycles. After measuring from the top, the samples were flipped over along their pinning axis as shown in Fig. 1. This way the easy direction remains the same, and hysteresis loops measured from both sides can be compared, since only the component of the magnetization along the applied field axis is of importance. Due to the attenuation of the light in the $Fe_{50}Mn_{50}$ layer, the major contribution to the MOKE signal originates from the top permalloy layer when measured from the top side and from the bottom permalloy layer when measured from the glass side. From these measurements the coercivity H_c and pinning field H_p for each permalloy layer can be determined independently.

III. RESULTS

In the apparatus described above, the PEM mixes *s*-polarized and *p*-polarized light. The electric field incident on the sample is:

$$\mathbf{E}_0=\begin{pmatrix}E_{p,0}\\E_{s,0}\end{pmatrix}=E_0\begin{pmatrix}1+e^{i\phi}\\1-e^{i\phi}\end{pmatrix}, \tag{1}$$

where the phase is modulated as $\phi=\phi_0\cos\omega t$.

The complex reflectivity matrix for the longitudinal Kerr effect is[10]

$$\mathbf{R}=\begin{pmatrix}\tilde{r}_p & \tilde{r}_{ps}\\ \tilde{r}_{sp} & \tilde{r}_s\end{pmatrix}=\begin{pmatrix}r_p e^{i\delta_p} & r_{ps}e^{i\delta_{ps}}\\ -r_{ps}e^{i\delta_{ps}} & r_s e^{i\delta_s}\end{pmatrix}, \tag{2}$$

where $\tilde{r}_p$ and $\tilde{r}_s$ are the ordinary Fresnel coefficients for *p*- and *s*-polarized light. The absolute values of the off-diagonal coefficients $\tilde{r}_{ps}$ and $\tilde{r}_{sp}$ are known to be linearly dependent on the component of magnetization in the applied field direction.

To model the optical response using Jones matrix formalism, the 4 nm Ta layer is treated in the thin film limit, since its thickness is much smaller than the wavelength of the incident radiation and it does not show any gyrotropic effect. The Kerr signals are assumed to originate from the air/permalloy and permalloy/glass interface. Moreover, we treat the trilayer as an effective medium, so the overall reflectivity is

$$\mathbf{R}=\mathbf{R}_1+\mathbf{T}_{21}\mathbf{R}_2\mathbf{T}_{12}\exp(-d/\delta)\cos\Delta, \tag{3}$$

where $\mathbf{R}_1$ denotes the reflection matrix at the first permalloy interface, $\mathbf{T}_{12}$, $\mathbf{T}_{21}$ are the transmission matrices, and $\mathbf{R}_2$ the reflection matrix at the second permalloy interface. The product $\mathbf{T}_{21}\mathbf{R}_2\mathbf{T}_{12}$ can be rewritten as an effective reflection matrix $\mathbf{R}_{2,\mathrm{eff}}$. The damping is assumed to be exponential, where δ is the skin depth of the effective medium, and Δ the phase difference accumulated by the light traveling through the medium that depends on the optical path length d in the multilayer $\Delta=n(2\pi/\lambda)d$. The exponential term is responsible for the damping, the cosine term for the oscillatory behavior.

The signal measured for a single layer is proportional to the square of the electric field amplitude. The signal for the *p*-polarized analyzer is

$$I=\tfrac{1}{2}[r_p^2+r_{ps}^2+(r_p^2-r_{ps}^2)\cos\phi - 2r_p r_{ps}\sin(\delta_p-\delta_{ps})\sin\phi]. \tag{4}$$

The trigonometric terms can be expanded into a series of trigonometric functions in $m\omega=2\pi mf(m=0,1,2,...)$:

$$\sin\phi=2\sum_{m=0}^{\infty}J_{2m+1}(\phi_0)\sin[(2m+1)\omega t], \tag{5}$$

$$\cos\phi=J_0(\phi_0)+2\sum_{m=0}^{\infty}J_{2m}(\phi_0)\cos[2m\omega t]. \tag{6}$$

The lock-in amplifier was set to the fundamental frequency, *f*, and the phase of the PEM set to $\phi_0=108°$, which maximizes the Bessel function $J_1(\phi_0)$. The recorded signal is in the linear approximation proportional to the ellipticity ϵ_K.[11]

$$V_f\propto -1.16[r_p r_{ps}\sin(\delta_p-\delta_{ps})] = -1.16r_p^2\,\mathrm{Im}\{r_{ps}/r_p\}\approx 1.16r_p^2\epsilon_K. \tag{7}$$

For the trilayer, the optical path length for the light reflected from the two permalloy layers is different. Since the incident radiation is coherent, the signal from the bottom layer has a nonzero phase relation to that from the top layer. When measured from the top the signal becomes

$$|\mathbf{E}|^2=|\mathbf{E}_T+a\mathbf{E}_B e^{i\Delta}|^2=\mathbf{E}_T^2+a^2\mathbf{E}_B^2+2a\mathbf{E}_T\mathbf{E}_B\cos\Delta, \tag{8}$$

where a denotes the exponential damping factor. The last term in Eq. (8) is the interference term. The top and the bottom layer may be in a different magnetic state, so the two off-diagonal coefficients $r_{ps,T}$ and $r_{ps,B}$ must be written out separately as well as the diagonal coefficients. The *p*-polarized component of the reflected light measured is

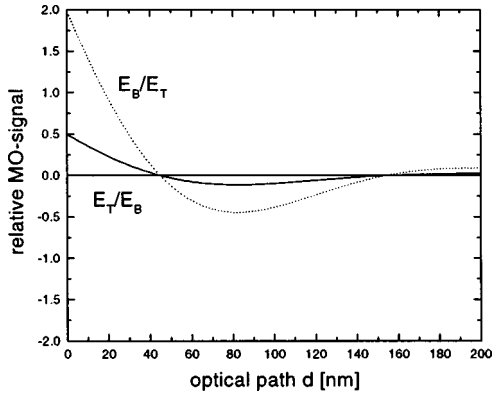

FIG. 2. Ratio of the MOKE signals from the top and bottom permalloy layer measured from the top (E_B/E_T) and from the bottom (E_T/E_B) vs optical path length, d. The oscillatory behavior is caused by optical interference, the damping by attenuation.

$$V_f \propto \left\{ \left[\mathrm{Im}\left(\frac{\tilde{r}_{ps,T}}{\tilde{r}_{p,T}}\right)(1+a\cos\Delta) + a\,\mathrm{Re}\left(\frac{\tilde{r}_{ps,T}}{\tilde{r}_{p,T}}\right)\sin\Delta \right] + \left[\mathrm{Im}\left(\frac{\tilde{r}_{ps,B}}{\tilde{r}_{p,B}}\right)(a\cos\Delta + a^2) - a\,\mathrm{Re}\left(\frac{\tilde{r}_{ps,B}}{\tilde{r}_{p,B}}\right)\sin\Delta \right] \right\} J_1(\phi_0). \quad (9)$$

This expression is related to the Kerr rotations θ_K and ellipticities ϵ_K of the two permalloy layers which are the real and imaginary parts of the off-diagonal components of the reflectivity tensor, respectively.[11] For $\lambda = 632$ nm, θ_K and ϵ_K for permalloy are nearly equal,[12] so that we can equate the real and imaginary parts in Eq. (9). Since the attenuation, a, is less than unity, the first term does not change sign with varying optical path, but the second term does. Thus the sense of the Kerr loops from the bottom layer will vary with the $Fe_{50}Mn_{50}$ thickness. From Eq. (9) the ratio of the MOKE signals is

$$\frac{E_B}{E_T} \approx \frac{t_B}{t_T}\,\frac{\exp(-d/\delta)[\exp(-d/\delta)+\cos(nkd)-\sin(nkd)]}{1+\exp(-d/\delta)[\cos(nkd)+\sin(nkd)]}, \quad (10)$$

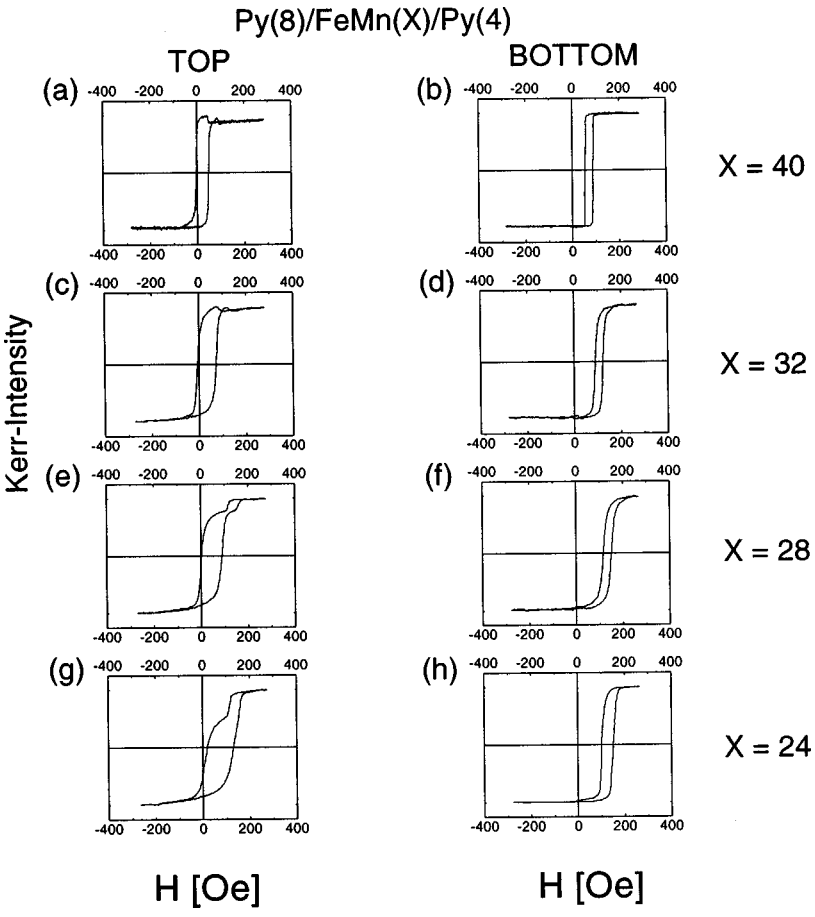

FIG. 4. Hysteresis loops measured with the longitudinal Kerr effect along the easy axis for permalloy (8 nm)/$Fe_{50}Mn_{50}(X)$/permalloy (4 nm) trilayers as a function of $Fe_{50}Mn_{50}$ spacer layer thickness.

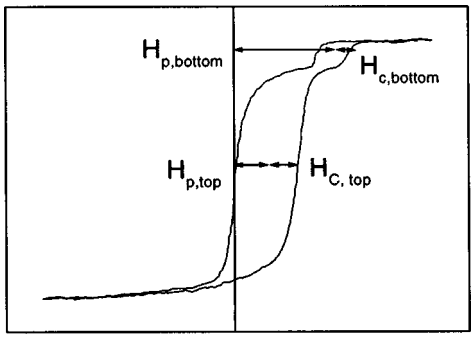

FIG. 3. Coercive fields H_c and pinning fields H_p for top and bottom layer can be extracted from the measured hysteresis loop.

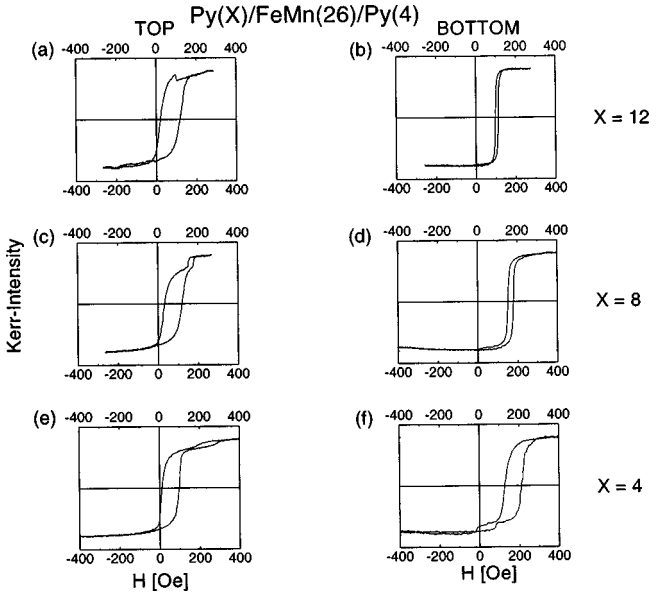

FIG. 5. Hysteresis loops measured with the longitudinal Kerr effect along the easy axis for permalloy $(X)/Fe_{50}Mn_{50}$ (26 nm)/permalloy (4 nm) trilayers as a function of permalloy thickness.

where t_T and t_B denote the thicknesses of the top and bottom permalloy layers, respectively. Here it is assumed that in the thin film limit the off-diagonal components of the reflectivity tensor increase linearly with the F layer thickness.[13] To obtain the ratio for the signal measured from the bottom one needs to interchange the subscripts T and B in Eq. (10). These ratios are plotted in Fig. 2 versus the optical path length d for $n=2.52$ and $\delta=60$ nm, which is in the order of the measured refractive indices and skin depths for permalloy ($n=2.42$, $\delta=58$ nm) and $Fe_{50}Mn_{50}$ ($n=2.18$, $\delta=52$ nm) obtained using a spectroscopic ellipsometer.[14] Here $t_B/t_t=2$ is assumed. The first reversal in sign occurs for an optical path length of 50 nm. The angle of refraction in the permalloy is about 15°, which corresponds to an angle of incidence of 45° used in the experiment. Thus an optical path length of $d=50$ nm corresponds to a 26 nm thick metallic layer. The hysteresis loops presented show how optical interference affects the observed response. The coercive fields H_c and pinning fields H_p for the top and bottom permalloy layer can be extracted from the measurement, since the signal from the bottom layer is attenuated, and the loop shift H_p differs from that of the top layer. A typical hysteresis loop for a trilayer is shown in Fig. 3.

The MOKE data for bottom permalloy (8 nm)/$Fe_{50}Mn_{50}(X)$/top permalloy (4 nm) samples with $X=24$, 28, 32, and 40 nm $Fe_{50}Mn_{50}$ spacer layers are shown in Fig. 4. Hysteresis loops measured from the top and bottom of the trilayer samples are presented in the left and right columns, respectively. While the major loops for the 24 and 28 nm $Fe_{50}Mn_{50}$ spacer show the ordinary stepped shape, which is a superposition of equally oriented loops originating from the top and bottom permalloy layers, the major loops for the 32 and 40 nm $Fe_{50}Mn_{50}$ spacer show a reversal in the sense of the hysteresis loop from the bottom layer. This can be attributed to the finite optical path length through the trilayer. By comparing the loops of the left and right column of Fig. 4, it

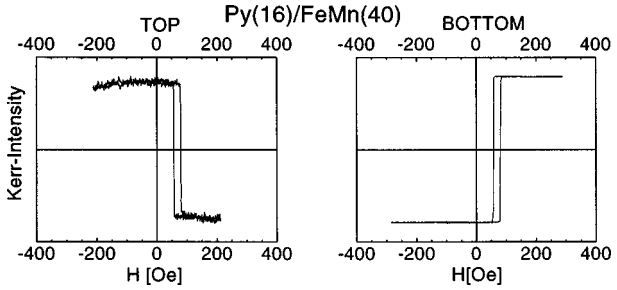

FIG. 6. Hysteresis loops measured for a permalloy (16 nm)/$Fe_{50}Mn_{50}$ (40 nm) bilayer. The reversal of the sense of the loop when measured from the top through the $Fe_{50}Mn_{50}$ is clearly observed.

can be found, that the switching field of the bottom permalloy measured from the top and bottom coincide. Vibrating sample magnetometer[15] data confirms the optical nature of this effect, since it shows that the magnetization of the bottom layer switches in the same direction as the top layer. The reversal occurs at a larger thickness than predicted by the model, which is not surprising considering the model is a first-order approximation that neglects Faraday rotation for light traveling through the permalloy and multiple internal reflections. The MOKE data for bottom permalloy $(X)/Fe_{50}Mn_{50}$ (26 nm)/top permalloy(4 nm) samples with $X=4$, 8, and 12 nm is shown in Fig. 5. A reversal in the hysteresis loop sense of the buried layer can be observed for the thickest layer of permalloy. The total thickness of the trilayer for which the reversal takes place is the same as is observed in the data of Fig. 4. This observation justifies the approach of treating the trilayer as an effective medium and shows that interference due to the finite optical path is the origin of the loop reversal. The reversal in the sense of the hysteresis loop is more readily observed for a single permalloy layer buried by a $Fe_{50}Mn_{50}$ layer. The MOKE data of a permalloy (16 nm)/$Fe_{50}Mn_{50}$ (40 nm) bilayer is shown in Fig. 6. The sense of the loop changes when measured from the air side or from the substrate side. However, since the loop can only originate from one layer, the variation of the optical path length for the two measurements is the only source of the loop reversal. The magnitude of the signal from the buried layer is reduced due to attenuation, and the sign of the signal is reversed due to interference. The first-order approximation explains the qualitative behavior of this observation.

IV. CONCLUSION

It has been demonstrated that the switching of buried magnetic layers can be observed with coherent MOKE. The reversal of the hysteresis loops of buried layers has its origin in the finite optical path length. A first-order approximation was presented which predicts that the MOKE signal contains both a damping term and an oscillatory term. The observed first zero crossing of the response occurs at a larger thickness than the simple model predicts. Possible sources of the difference could be due to the Faraday rotation of the light through traveling through the permalloy layers, treating the

trilayer as an effective medium, and multiple internal reflections. A more rigorous treatment would include the full matrix calculation by matching boundary conditions of the Maxwell equations at each interface.[13,16,17]

ACKNOWLEDGMENTS

This work was supported by grants from the National Science Foundation, DMR-9400399, and the Army Research Office, DAAH 04-94-6-0251 and DAAH 04-96-1-0316.

[1] B. Dieny, V. S. Speriosu, S. S. P. Parkin, B. A. Gurney, D. R. Wilhoit, and D. Mauri, Phys. Rev. B **43**, 1297 (1991).
[2] K. T.-Y. Kung, L. K. Louie, and G. L. Gorman, J. Appl. Phys. **69**, 5634 (1991).
[3] G. Penissard, P. Maeyer, J. Ferre, and D. Renard, J. Magn. Magn. Mater. **146**, 55 (1995).
[4] J. Ferre, P. Meyer, N. Nyvlt, S. Visnovsky, and D. Renard, J. Magn. Magn. Mater. **165**, 92 (1997).
[5] R. Jerome, T. Valet, and P. Galtier, IEEE Trans. Magn. **30**, 4878 (1994).
[6] A. Choukh, IEEE Trans. Magn. **33**, 3676 (1997).
[7] C. Hwang, R. H. Geiss, and J. K. Howard, J. Appl. Phys. **64**, 6115 (1988).
[8] H. Umebayashi and Y. Ishikawa, J. Phys. Soc. Jpn. **21**, 1281 (1966).
[9] P. Q. J. Nederpel and J. W. D. Martens, Rev. Sci. Instrum. **56**, 687 (1985).
[10] R. P. Hunt, J. Appl. Phys. **38**, 1652 (1967).
[11] M. Mansuripur, *The Physical Principles of Magneto-optical Recording* (Cambridge University Press, Cambridge, 1995).
[12] A. Berger and M. R. Pufall, Appl. Phys. Lett. **71**, 965 (1997).
[13] J. Zak, E. R. Moog, C. Liu, and S. D. Bader, J. Magn. Magn. Mater. **89**, 107 (1990).
[14] Variable angle spectroscopic ellipsometer, J.A. Woollam Co., Inc., Lincoln, NE.
[15] Vibrating sample magnetometer model 1660, Digital Measurement Systems, Burlington, MA.
[16] J. Zak, E. R. Moog, C. Liu, and S. D. Bader, Phys. Rev. B **43**, 6423 (1991).
[17] P. Yeh, Surf. Sci. **96**, 41 (1980).